Chapter 7

Magnetic-ordering of the epitaxial Thulium Iron Garnet thin film

abstract

Magnonics has shown the immense potential of substituting CMOS devices with lower energy-consuming devices and the ability to be utilized in futuristic quantum computing [237, 238]. Therefore, metallic and insulating magnonic materials are being extensively explored. High spin-orbit interaction (SOC) induced by rare-earth elements in TmIG increases its potential in spintronics and magnonic applications. High SOC materials with Pt, Ta, and W interfaces exert a force on the magnetic material when an electric current is applied. This is known as spin-orbit torque (SOT). SOTs can cause magnetic switching in an ultra-fast regime, making TmIG a potential conduit in spintronics. With this possibility of electrically excited and detected spin waves using the SOTs, it has application in magnonics. Here, we present a cost-effective solution-based approach that enables the excellent quality interface and surface roughness of the epitaxial TmIG/GGG.

The deposited TmIG (12 $\pm$ 1 nm) thin film's physical and spin dynamic properties are investigated in detail. The confirmation of the epitaxy was obtained using X-ray diffraction in ϕ-scan geometry along with the X-ray reflectivity and atomic force for the thickness, roughness analysis, and topography, respectively. The epitaxial TmIG/GGG films have the perpendicular magnetic anisotropy confirmed utilizing the polar-magneto-optic Kerr effect. Analyzing the FMR study of TmIG/GGG thin films provides the anisotropy constant K = 20.0 $\pm$ 0.3 kN/m^2 and the Gilbert damping parameter α = 0.018 $\pm$ 0.004. The experimental findings suggest that the solution-processed TmIG/GGG thin films with improved developing environment can be utilized in device applications.

7.1 Introduction

Magnonics is the study of spin waves-based information processing and transmission [239]. Magnons can be utilized in more dense logic gates, along with the processing and transporting of information simultaneously [17]. Magnon's superposition makes it a potential candidate for its uses as a qubit in quantum computing [240]. There are various magnon carrier systems; some are conducting, and others insulating [17]. Conducting magnonic materials are CoFeB [241, 242], NiFe(Permalloy) [243, 244], and Heusler compounds [245, 246]. Iron garnets are one class of these insulating magnonic materials [18]. Various fundamental understandings of magnon behaviors like magnon-magnon scattering and magnetic resonance have been considered possible microscopic origins using these ferrimagnetic insulators [83, 26]. Recently, the heterostructure YIG was found to be applicable to spin pumping [185, 196]. Soon after its discovery in the 1950s, the experimental study confirmed that the system had the lowest dissipation (lowest linewidth of the FMR), making it a promising system for various applications [247]. A recent study shows that in PLD grown Pt/YIG, the interfacial spin Hall angle (θ_{SH}) is 0.33 [33]. Further advanced processing can be achieved by PMA in the system [248]. YIG

has a low anisotropy constant $K_U = 1\times10^3$ N/m^2 when deposited on GGG substrate [249]. High spin-orbit coupling in rare-earth iron garnets has the potential to resolve the lower magnetic anisotropy in the thin films [250]. Complete substitutional rare-earth series can form in the iron garnets [206]. The rare-earth elements have their unique magnetic ordering, contributing to ferrimagnetic coupling. This ferrimagnetic ordering causes a compensation temperature, which is the lowest magnetization state. Thulium iron garnet (TmIG) is the rare-earth garnet with Curie temperature ($T_C \approx 550$ K [15]) with the lowest compensation temperature ≈15 K [124] and room temperature moderate saturation magnetization. Recently, the Pt/TmIG heterostructure with PMA shows the magnetic switching and spin magnetoresistance [251], and TmIG/Au/TmIG shows the spin valves properties [35].

Iron garnet thin films are grown using ultra-high vacuum facilities and require sophisticated instrumentation like PLD [252], rf-sputtering [236], and LPE [253]. A few studies have produced polycrystalline iron garnets using solution methods like spin-coating [50, 124, 45]. However, epitaxial thin film growth using spin-coating has not been reported to date. This work presents a cost-effective, all-solution-based spin-coating method that uses the substrate's crystal structure to reference and grows an epitaxial thin film of TmIG/GGG. The epitaxial TmIG/GGG has been studied using synchrotron GIXRD. The confirmation of the epitaxy was presented using GIXRD ϕ-scan. The topography and elemental analysis of TmIG magnonic material are studied in detail. The magnetic study confirms the high magneto-crystalline anisotropy in the deposited thin film caused by the high lattice mismatch that results in the PMA.

7.2 Results and discussion

7.2.1 Structural Study

The phase information of the TmIG thin film deposited using sol-gel-based spin coating was performed using the GIXRD. Highly monochromatic synchrotron X-rays of the 1.25 Å wavelength were utilized to resolve the thin film Bragg's reflection from the substrate reflection. Figure (7.1)(a) presents the out-of-plane XRD of TmIG (444) reflection with the substrate GGG (444) highest intensity reflection. Inset Figure (7.1)(a) shows the logarithmic plot of the intensity to show the excellent interface quality that confirms high crystallinity due to the presence of Laue oscillations [254]. The interplanar distance of GGG (444) and TmIG (444) are 1.794 $\pm$ 0.009 Å, and 1.778 $\pm$ 0.008 Å, respectively. The lattice constants are 12.38 $\pm$ 0.01 Å, and 12.26 $\pm$ 0.01 Å, respectively, for the GGG and TmIG. Experimental data confirm the smoothness of the interface and the epitaxial growth between the substrate and thin film, as shown in Figure 7.1 (b). The strain because of the mismatch between the two $\Delta\varepsilon = \frac{a_{GGG} - a_{TmIG}}{a_{GGG}}$ is 0.91 % which shows the tensile strain on the layer of TmIG thin film. The tensile strain is the cause of the presence of the PMA in the sample (discussed in further sections). Figure 7.1 (b) represents the ϕ-scan of the TmIG thin film. The ϕ-scan was measured along the (008) Bragg reflection, which is ψ = 54.7° from the (111) Bragg reflection [255]. The three-fold symmetry in the ϕ-scan can be observed in Figure (7.1)(c). The angle difference of 120^0 between three-fold symmetry is experimentally observed in ϕ-scan, which confirms the epitaxy of the deposited thin film [256]. The stress (σ) at the interface is calculated using the following equation [257]:

$$\sigma = \frac{Y}{1-\nu}\Delta\varepsilon \tag{7.1}$$

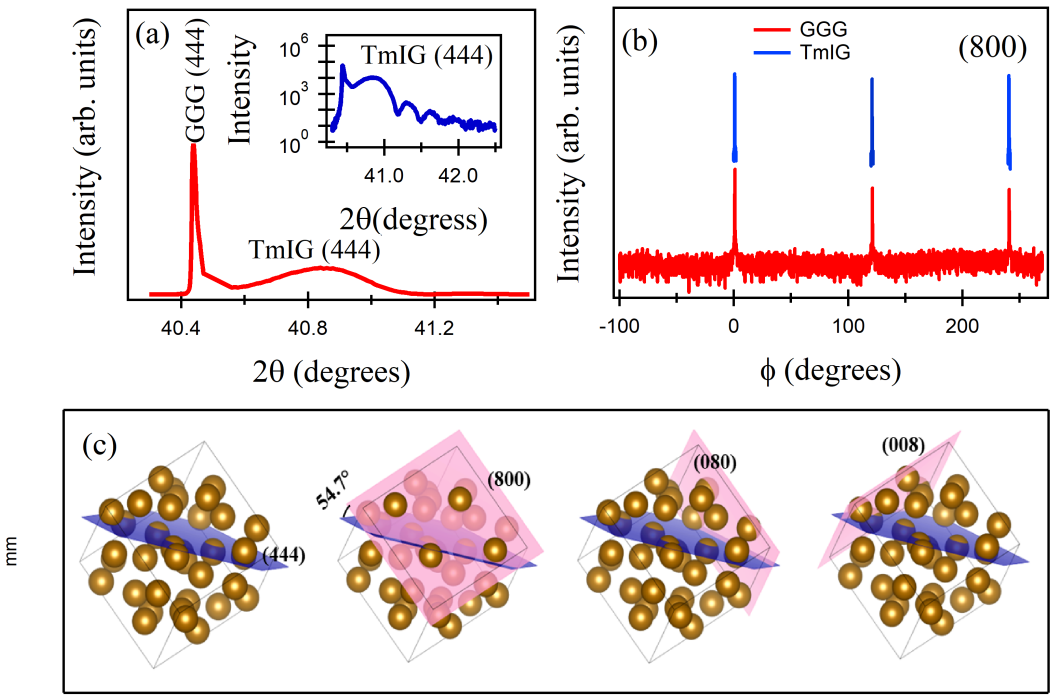

Fig. 7.1 *Structural confirmation of the epitaxial TmIG thin film deposited using all-solution-based spin-coating. (a) $\theta - 2\theta$ scan of GIXRD of the substrate and the thin film with the logarithmic inset to present excellent crystallinity, (b) ϕ-scan to confirm the epitaxy with the three-fold symmetry of the (008) plane and (c) schematic of the three-fold symmetry in 008 planes, golden spheres are the Tm^{3+} cations intersected by the growth direction of the thin film (444). Another family of planes 008 (in [pink color]) has been presented, showing the three-fold symmetry for the (444) plane.*

where, Y is Young's modulus (2.00×10^{11}N/m^2) and the ν is Poisson's ratio (0.29) as present in literature [206]. The σ calculated is $3 \pm 0.002 \times 10^9$ N/m^2.

7.2.2 Thickness and Topography Study

The substrate film interface quality is essential for the magnonic application as the interface roughens can tune the magnonic band gap of the materials [258]. Figure (7.2) illustrates the topography and structural quality of the deposited thin film using AFM and XRR. Figure (7.2)(a) illustrates AFM showing smooth topography, estimating mean roughness is 0.8 ± 0.1 nm. Along with the smooth surface are some spikes on the surface. These spikes

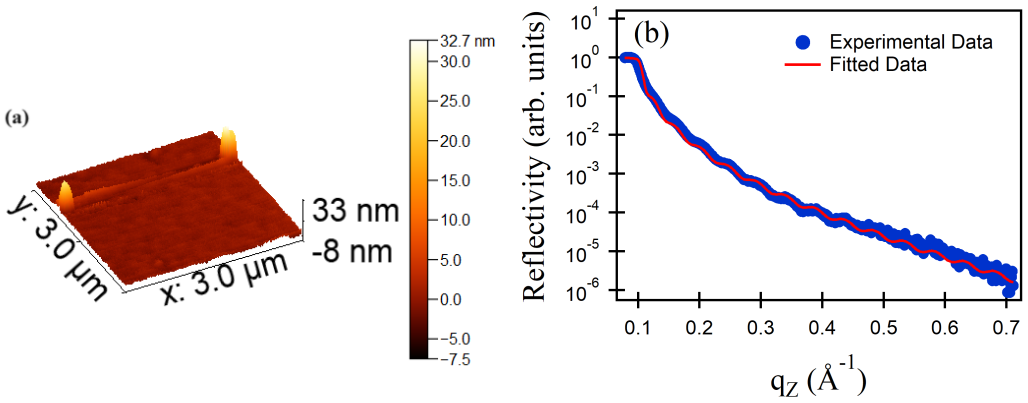

Fig. 7.2 *Surface topography and the thickness and roughness study estimation of epitaxial TmIG using (a) atomic force microscopy and (b) X-ray reflectivity.*

arise from the crystal growth phenomenon of the defect centers in the substrates, similar to the YIG/GGG thin films [210]. Figure (7.2)(b) illustrates the XRR of the TmIG thin film fitted using Parratt's formalism and that estimated the thickness of the 12.2 $\pm$ 1 nm, and the interfacial roughness 0.2 $\pm$ 0.1 nm, which is excellent. The degree of the crystallinity can also be accessed using the presence of Laue oscillations in the inset of Figure (7.1)(a). The surface roughness estimated is 0.4 $\pm$ 0.1 nm, which is in order equivalent to surface roughness estimation using AFM. The topography of the deposited thin film is smooth and suggests homogeneous growth on the substrate. Low surface and interface roughness show the potential of the sol-gel-based spin-coating method to study further applications.

7.2.3 Elemental Study

The elemental composition was probed using XPS. Figure (7.3): depicts the survey scan and the high-resolution XPS of the TmIG thin film. Figure (7.3)(a): plot the survey scan, giving the presence of O, C, Fe, Tm, and N in the thin film. The sample constituted O, Fe, and Tm, but the environmental exposure caused the C and N absorption. The sample was calibrated using the carbon at peak position 284.2 $\pm$ 0.1 eV. Figure (7.3)(b) illustrates the high-resolution spectra of the oxygen 1s core electrons. The main peak at binding energy

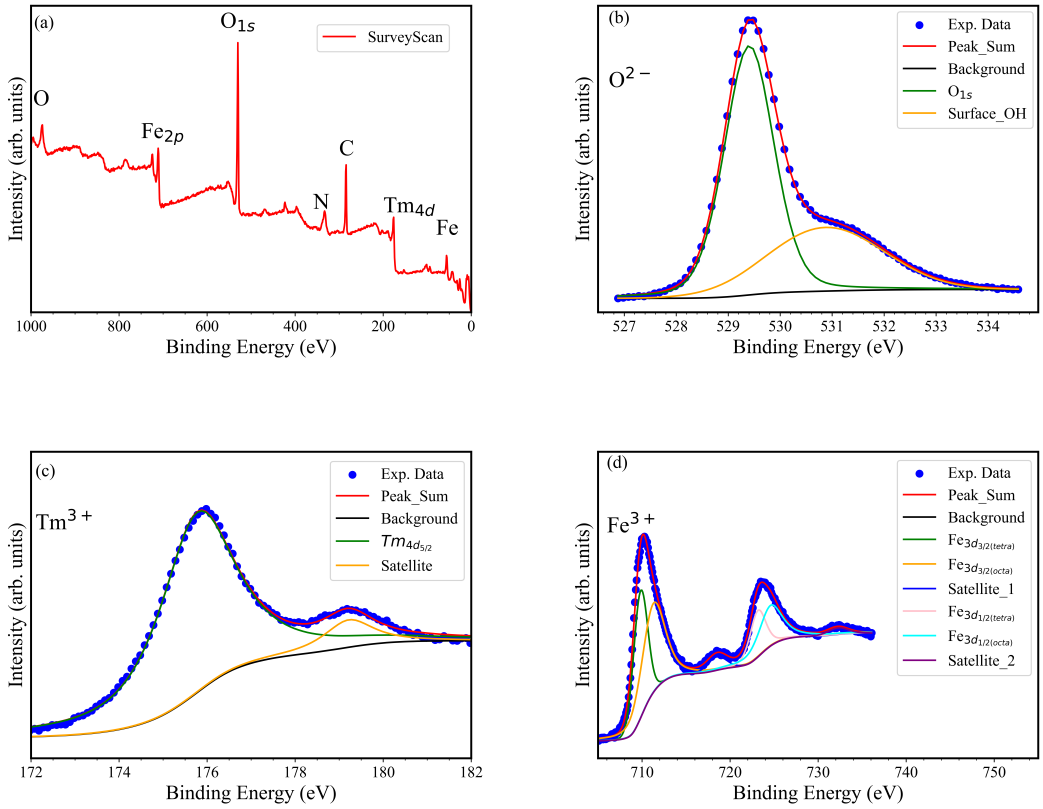

Fig. 7.3 *XPS of the TmIG thin film has been presented. (a) survey scan from binding energy 0-1000 eV. High-resolution XPS of the elements (b) O^{2-}, (C) Tm^{3+}, and (d) Fe^{3+} are fitted and presented with peak component with the Shirley background.*

529.4 $\pm$ 0.1 eV is because the O_{1s} electrons bind in the TmIG; along with this, the surface contribution of the oxygen is also there at 530.8 $\pm$ 0.1 eV. Figure (7.3)(c) illustrates the high-resolution spectra of thulium $4d_{5/2}$ core electrons. $Tm_{4d_{5/2}}$ is observed at 175.7 $\pm$ 0.1 eV which is supported by the literature [227]. Thulium is present in Tm^{2+} and Tm^{3+} but the most stable valence state is Tm^{3+}. The presence of a satellite peak at 179.2 $\pm$ 0.1 is similar to the literature and confirms Tm^{3+} charge state [259].

Figure (7.3)(d) illustrates the high-resolution spectra of the iron 2p core electrons. Iron is present in a 2:3 ratio of octahedral and tetrahedral coordinates in TmIG (space group $Ia\bar{3}d$). Therefore, the Fe $2p_{3/2}$ and $2p_{1/2}$ peak comprise two peaks each. The Fe octahedral (Fe_{oct})

peaks $2p_{3/2}$ at binding energy 709.8 $\pm$ 0.1 eV and $2p_{1/2}$ at binding energy 723.1 $\pm$ 0.1 eV. The Fe tetrahedral (Fe_{tetra}) peaks $2p_{3/2}$ at binding energy 711.2 $\pm$ 0.1 eV and $2p_{1/2}$ at binding energy 724.5 $\pm$ 0.1 eV. The theoretical ratio between the area of octahedral and tetrahedral Fe is 2:3. The experimental ratio of the area of peak $Fe_{2p_{3/2}}$ octahedral and tetrahedral Fe is 0.66, and of peak $Fe_{2p_{1/2}}$ octahedral and tetrahedral Fe is 0.83 [166]. The ratio is very close to the theoretical ratio 2:3, confirming that the ionic ordering of the film is as expected for TmIG [166]. The difference between the core electron peak and the satellite peak is large, 8 eV, which further establishes that Fe is in a 3+ valence state and the stoichiometry is balanced [124]. The atomic percentage of the constituents Tm^{3+}, Fe^{5+} and O^{2-} are 16 %, 26%, and 58%, respectively. The atomic percent is calculated using the CASAXPS software and is close to the 3:5:12 ionic ratio [169].

7.2.4 Magnetic Study

As the TmIG has application in magnonics, the magnetic properties of the deposited sample determine its application potential. Figure (7.4) presents the magnetic behavior of the deposited all solution-based epitaxial TmIG thin film at room temperature. Figure (7.4)(a) illustrates the polar MOKE measurements. The presence of out-of-plane total anisotropy gives the MOKE signal, which confirms the existence of the PMA at room temperature in the thin film [66]. The total anisotropy (K) in the thin film is a combination of various components like stress-induced anisotropy (K_σ), magneto-crystalline anisotropy (K_M), and shape anisotropy (K_S) [63]. Figure (7.4)(b) illustrates the schematics of the PMA in the film. The stress-induced anisotropy is calculated using the formula as follows:

$$K_\sigma = -\frac{3}{2}\lambda_{111}\sigma \tag{7.2}$$

where, λ_{111} is the magnetostriction constant (-5.2 $\times 10^{-6}$) of the TmIG as present in literature [206]. The value of the estimated stress-induced anisotropy (K_σ) is 20.07 $\pm$ 0.06 kN/m^2. Shape anisotropy (K_S) was estimated by square rooting the M_S for the continuous film and its value is 0.49 $\times 10^3$ N/m^2 [206]. The cubic anisotropy constant (K_1) value is taken from the literature [66] is -1.1$\times 10^3$ N/m^2. The final total anisotropy value is estimated as follows:

$$K = K_1 + K_\sigma + K_S \tag{7.3}$$

The estimated K from the strain is 19.5 $\times$ kN/m^2.

The FMR-based magnetic study of the TmIG also included as it probes the precession of the moments along the effective field, and this precession resonates at a given field for the applied microwave frequency. The absorption of energy at that frequency at a particular magnetic field gives the resonance magnetic field and the linewidth of the absorption, which signifies the moment's precession and energy dissipation, respectively. Figure (7.4): depicts the FMR results, (a) plots in-plane the resonance magnetic field (H_{res}) as a function of frequency and fitted using Kittel equation, (b) illustrates the linewidth as a function of the frequency. Kittel equation [164, 260] is as presented below:

$$f = \left(\frac{\gamma}{2\pi}\right)\sqrt{H(H+\mu_0 M_{eff})} \tag{7.4}$$

The effective magnetization ($\mu_0 M_{eff}$) estimated is -0.281 $\pm$ 0.004 T. As the PMA is confirmed with the polar MOKE, the negative value of $\mu_0 M_{eff}$ shows that anisotropy dominates the saturation magnetization. $\mu_0 M_{eff}$ is composed of saturation magnetization ($\mu_0 M_S$) and the anisotropy field (H_U) in following equation[63]:

$$\mu_0 M_{eff} = \mu_0 M_S - H_U \tag{7.5}$$

In the literature, the saturation magnetization value ($\mu_0 M_S$) of bulk TmIG is 0.1244 T [236]. The anisotropy Field (H_U) is estimated to be 0.4167 T. The anisotropy constant (K) is calculated by substituting the anisotropy field and saturation magnetization as present in the following equation:

$$K = \frac{H_U \times M_S}{2} \tag{7.6}$$

K is estimated by substituting; the value is 20.0 ± 0.3 kN/m^2. K estimation by FMR is equivalent to the K calculated with the strain in GIXRD. This value is higher than the literature due to the self-growth of the TmIG/GGG and forms a better interface. The value of the gyromagnetic ratio is 19.0 ± 0.2 GHz/T, which is lower than the free electron because of the high spin-orbit coupling of the thulium ions. The g-factor estimated is 1.36 ± 0.01 from the gyromagnetic ratio. The g-factor is smaller than the free electron and the value present for TmIG in literature [260]. The significant deviation between the g factor and the electron spin g-factor of value $\approx$2 is because of the high SOC of the Tm atom. The high SOC causes the mixing of the orbital magnetism, giving rise to the lower energy separation and, thus, the lower g-factor [261, 262]. The presence of a low g-factor can also be due to the high anisotropy in TmIG/GGG thin film [263]. The uniform mode is generated while the moment precession relaxes by the dissipating energy due to extrinsic and intrinsic factors. Extrinsic factors are like defects and two-magnon interaction. Intrinsic factors are like electron-electron interaction and high spin-orbit interaction. These factors can be obtained from the linear fitting of the magnetic linewidth as a function of the applied frequency. Figure (7.4)(d) depicts the linewidth (ΔH) as a function of the applied frequency. Blue dots are obtained by analyzing the experimental FMR data as a function of the applied field (the intensity of the dP/dH is low, which causes the deviation), and the red line fits them linearly. The relation of linewidth, intrinsic, and extrinsic damping parameters is as follows:

$$\Delta H = \Delta H_0 + \frac{4\pi\alpha}{\gamma} f \tag{7.7}$$

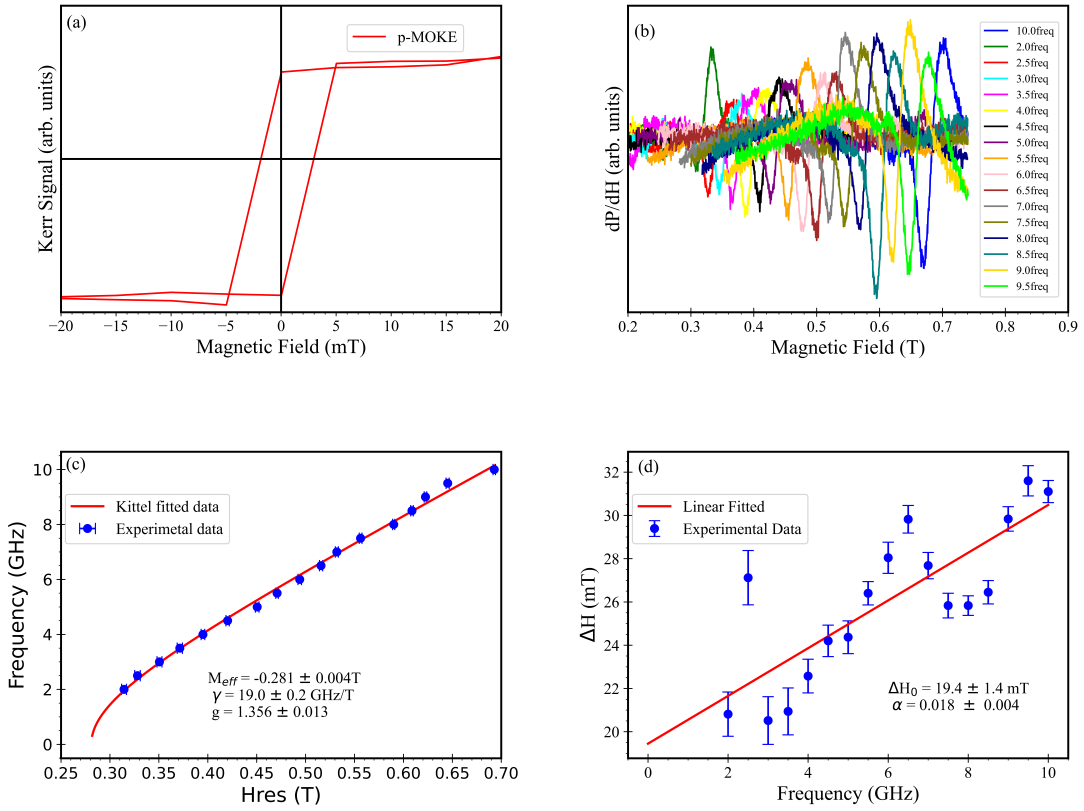

Fig. 7.4 *FMR study of the TmIG/GGG thin film (a) polar MOKE of the TmIG at room temperature, (b) first derivative of the phase as the function of the applied field at frequency range 2 - 10 GHz (c) Kittel fitting to the resonance magnetic field to study effective magnetic field and gyromagnetic ratio. (d) Linear fit to the linewidth as a function of frequency.*

The ΔH_0 is the inhomogeneous part of the TmIG energy dissipation, and the fitted value is the ΔH_0 is 19 $\pm$ 1 mT. The Gilbert damping parameter is intrinsic dissipation (α) = 0.018 $\pm$ 0.004. However, nonlinearity in data is not clear. It could be the broadband FMR's lower power or the growth spikes that give rise to this as an error. This can be understood as future work on the sol-gel-based spin coating epitaxial TmIG. Further studies like The Gilbert damping parameter are in the same order as in literature in which samples are prepared with sophisticated methods [66]. The non-linear linewidth results from the magnon-magnon scattering in the TmIG/GGG thin film because of the crystal growth as some defect centers, as presented in the AFM.

Table 7.1 *The comparison of the present deposited TmIG/GGG with the literature.*

Substrate	Deposition Method	Thickness (nm)	Damping Parameter	Anisotropy constant (10^3 N/m^2)	reference
GGG (111)	Sol-gel-based Spin-coating	12.2	0.018	20.0	present
GGG (111)	PLD	29	0.013	9	[264]
GGG (111)	PLD	20 - 300	0.02	10	[64]
GGG (111)	sputtering	9	0.013	-	[236]
GGG (111)	PLD	8	-	11.88	[66]

This thesis presents a cost-effective method, and to understand its potential, the literature is compared with the present work in table 7.1. All the samples are grown on the GGG (111) substrate, and the thicknesses are different, but the Gilbert damping parameter varies from 0.02-0.013. The estimated K is higher than the literature, giving this method another argument to explore further [149, 265].

7.3 Summary

Sol-gel-based spin coating deposits the epitaxial TmIG thin film on the GGG substrate. The elemental analysis confirms the stoichiometric deposition with low interface and surface roughness. The perpendicular magnetic anisotropy of this all-solution method deposited TmIG due to the stress-induced anisotropy. The high spin-orbit coupling gives rise to the lower gyromagnetic ratio and g-factor, which is well matched with the literature [261, 262]. The intrinsic and extrinsic dissipation factors of TmIG present a potential for the deposition method. This cost-effective deposition method can potentially be used for magnonics applications with further improvements in the deposition conditions and the controlled environment.